Research Square

Preprints are preliminary reports that have not undergone peer review.
They should not be considered conclusive, used to inform clinical practice,
or referenced by the media as validated information.

Fatigue Life Prediction for Gas Turbine Bearing Under 3D Elastoplastic Mixed Lubrication Condition

Yan Feng
Harbin Engineering University
Xiujiang Shi (shixiujiang@163.com)
Harbin Engineering University
Xiqun Lu
Harbin Engineering University
ZhuoYi Qiu
Harbin Engineering University
Wen Sun
Harbin Engineering University
Deliang Hua
Harbin Engineering University
Renze Li
Harbin Engineering University

Original Article

Keywords: Gas Turbine Bearings, Elastoplastic Deformation, Machined Roughness, Relative Fatigue Life

Posted Date: January 25th, 2021

DOI: https://doi.org/10.21203/rs.3.rs-151160/v1

License: This work is licensed under a Creative Commons Attribution 4.0 International License.
Read Full License

Fatigue Life Prediction for Gas Turbine Bearing under 3D Elastoplastic Mixed Lubrication condition

Yan Feng, Xiujiang Shi*, Xiqun Lu, ZhuoYi Qiu, Wen Sun, Deliang Hua, Renze Li
College of Power and Energy Engineering, Harbin Engineering University, Harbin, Heilongjiang, 150001, China

Abstract

Gas turbine bearings usually work in harsh lubrication environments, with typical characteristics such as high speed, high temperature, and heavy load. Severe working conditions bring micro-contacts in local areas between the bearing rolling elements and the rings. Stress concentration and plastic deformation may further occur between the contact pairs, which will reduce the fatigue life of the bearing. In order to predict bearing fatigue life accurately, in this study, the effects of the real surface roughness and plastic deformation of the bearing are considered, a three-dimensional(3D) elastoplastic mixed lubrication model for gas turbine bearing is established, the 3D dynamic elastoplastic stress calculations under the surface are conducted, and the relative fatigue life of the bearing is predicted. Based on the 3D elastoplastic mixed lubrication model for the bearing, the influences of speed, load, roughness and material hardening on lubrication performance and fatigue life are also studied, which would provide theoretical guidance for the lubrication design and life prediction of the gas turbine bearings.

Keywords: Gas Turbine Bearings, Elastoplastic Deformation, Machined Roughness, Relative Fatigue Life

Nomenclature

W	Normal load, N	η	Film viscosity, Pa·s
k	Ellipticity ratio	ε^P	Plastic strain
R_x, R_y	Radius of curvature in the x and y direction, m	p	Film pressure, Pa
δ_i	Real machined surface roughness, m	h, h_{min}	Film thickness and minimum film thickness, m
v_e	Elastic deformation, m	v_p	Plastic deformation, m
R_q	Root mean square (RMS) of the surface roughness, m	R_a, R_t	Statistic arithmetic mean roughness and total height between the peak and the valley, m
σ_{vm}	Von Mises stress, Pa	D_m	Pitch circle diameter, m
D_{r1}, D_{r2}	Diameter of the outer raceway and inner raceway, m	U_1, U_2	Velocity of the bearing rolling element and the inner raceway, m/s
U	Entrainment velocity along the	x,y,z	Fixed coordinate system

	rolling direction, m/s		for the bearing
ES	Relative plastic modulus	E	Young's modulus, Pa
E_{Ts}	Tangent modulus, Pa	ρ	Density of the lubricant, kg/m^3
σ_{Y0}	Initial yield limit, Pa	a, b	Hertz contact length in the x and y direction, m
M_R	Stress volume integral ratio	$Vol(\sigma_{eq})$	Stress volume integral
N, M, L	The number of grid nodes along x, y and z directions in the calculated region	L_R	Relative fatigue life

1. Introduction

In recent years, gas turbines have developed with the trend of "low consumption, high supply, and long life" [1-2]. As one of the main transmission components of the gas turbine, the rolling bearing is also one of the most vulnerable parts of a gas turbine, due to the severe running environments. Harsh working conditions such as high temperature, high pressure, high speed, and heavy load often lead to an extremely thin oil film between the contact interfaces, deterioration of lubrication conditions, and even local roughness contact, which can further bring stress concentration, plastic deformation, fatigue pitting and other failure modes. Therefore, in order to perform mixed lubrication numerical analysis and predict the fatigue life of gas turbine bearings accurately, it is necessary to consider the effects of the real rough surface and plastic deformation.

The fatigue life prediction considering surface topography has attracted lots of attention from many scholars in the past decades. Akamatsu [3] and Zhai [4] carried out an experimental study on the effect of surface skewness on fatigue life, and revealed that reducing friction coefficient can prolong fatigue life. Zhu et al. [5] proposed a line contact optimization material constant model for real machined 3D rough surface, which can well predict the pitting life by comparing with experimental data. Xiaoliang Yan et al. [6-7] considered the influence of roughness parameters, skewness, kurtosis and morphology on the mixed hydrodynamic contact fatigue life, and showed the conclusion that the skewness increases and the kurtosis decreases will cause local stress concentration and reduce fatigue life. Considering the effect of real rough surface of the rolling bearing, 315 simulation cases under heavy-load conditions had been calculated, Yadi Lu[8] concluded that heavy load will cause subsurface stress concentration and further affect bearing life.

The effect of plastic deformation on fatigue life has also attracted much attention in recent years. Oswald et al. [9] incorporated the effects of residual and hoop stresses of rolling bearing fatigue life based on Zaretsky life equation were studied. Donglong Li[10], based on the experimental research of the rolling contact fatigue test was investigated by Xie et al. [11] established a three-dimensional elastoplastic rolling contact model, and the experimental results show that the greater the hardness of the material at the position where maximum residual stress occurs, the longer the fatigue life. Chao Pu et al. [12-13] analyzed the influence of cracks on elastoplastic lubrication performance of deep groove ball bearings, and solved the heavy load problem with semi

analytical method, which greatly improved the calculation efficiency. Xin Lu[14] predicted the elastic-plastic low cycle fatigue life of aerospace bearings by using the finite element method, and revealed the relationship between cumulative plastic deformation and fatigue life. Harati et al. [15] after fatigue testing of the weld toe proposed that the fatigue life of weld toe can be improved by proper residual stress.

As shown, the fatigue life based on mixed EHL research considering surface roughness and the elastoplastic lubrication studies in point-contact have been reported widely. However, few studies focus on the fatigue life prediction of the bearings considering the machined 3D surface roughness and plastic deformation at the same time, especially for the bearings in gas turbine fields. Therefore, in this study, the gas turbine bearing is taken as the research case, considering the influences of real surface roughness and plastic deformation, a 3D elastoplastic mixed lubrication model is established to predict the fatigue life of the gas turbine bearing.

2. Numerical modeling of elastoplastic fatigue life of gas turbine bearing

2.1 Bearing structure model

In the ball bearing as shown in Fig. 1, the severe lubrication usually occur between the balls and the races, and further affect the fatigue life. As shown in the figure, D_m is the pitch circle diameter of the bearing, which is equal to the average diameter of the inner and the outer raceway, namely,

$$D_m = 0.5(D_{r1}+D_{r2}). \quad (1)$$

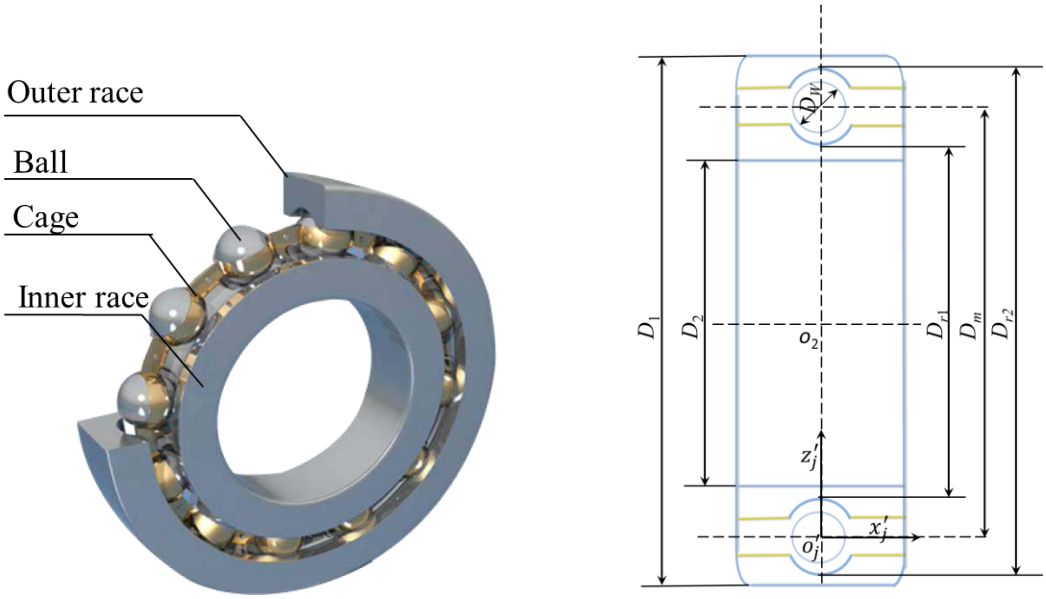

Fig. 1. Gas turbine and gas turbine bearing plan.

In order to calculate the lubrication state accurately, firstly, the lubrication model for ball-race contact needs to be built. The equivalent lubrication model between the ball and the inner raceway is taken as a case and shown in Fig. 2. For the rolling elements, the ball radii in the $x_{2j}o_{2j}z_{2j}$ plane and $y_{2j}o_{2j}z_{2j}$ plane are the same as shown in Figs. 2(c) and (d), which are calculated as is as,

$$R_{x2jj} = R_{y2jj} = \frac{D_W}{2} \quad (2)$$

For the bearing inner raceway, the radii of curvature in the x_{2j} and y_{2j} directions are different. The radii in the $x_{2j}o_{2j}z_{2j}$ and $x_{2j}o_{2j}z_{2j}$ planes are expressed as,

$$R_{x_{2j}2} = \frac{D_m - D_W \cos\alpha_{2j}}{2\cos\alpha_{2j}} \quad (3) \qquad R_{y_{2j}2} = f_i D_W. \quad (4)$$

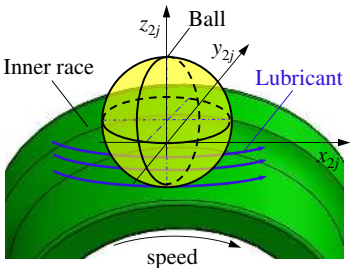

(a) Contact model between ball and inner ring

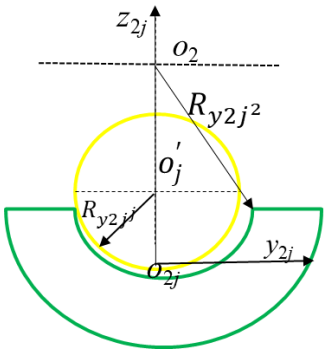

(b) Concave contact in the y_{2j} direction

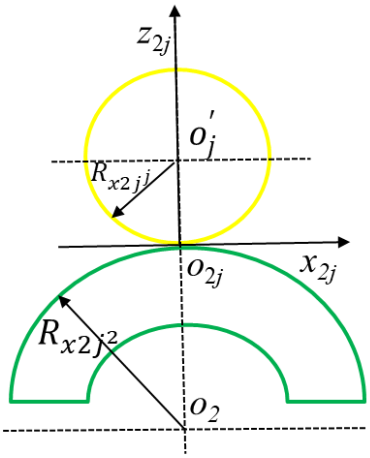

(c) Convex in the x_{2j} direction

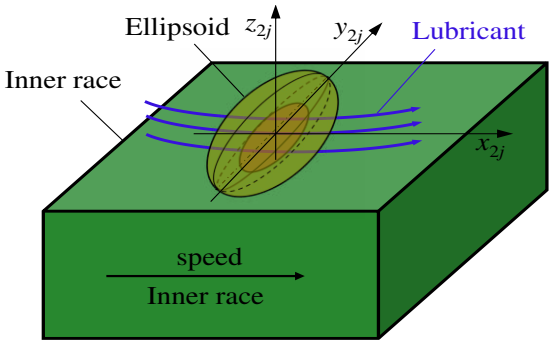

(d) Contact equivalent model.

Fig. 2. Contact equivalent diagram of rolling element and inner ring.

2.2 Lubrication equation with Elastoplastic deformation and real surface roughness

The real surface roughness and elastoplastic deformation can affect the film thickness clearly, for solving the bearing lubrication state more accurately, the following film thickness equation between the ball and the race is employed as,

$$h = h_0 + \frac{{x_{2j}}^2}{2R_{x2j}} + \frac{{y_{2j}}^2}{2R_{y2j}} + v_e(x_{2j}, y_{2j}, t) + v_p(x_{2j}, y_{2j}, t) + \delta_1(x_{2j}, y_{2j}, t) + \delta_2(x_{2j}, y_{2j}, t) \quad (5)$$

Where v_e is the Elastic deformation of the ball and race and can be calculated as,

$$v_e\left(x_{2j}, y_{2j}, t\right) = \frac{2}{\pi E'} \iint_{\Omega} \frac{p(\xi,\zeta,t)}{\sqrt{(x_{2j}-\zeta)^2 + \left(y_{2j}-\xi\right)^2}} d\zeta d\xi. \quad (6)$$

And v_p is the surface plastic deformation, which is expressed as,

$$v_p\left(x_{2j}, y_{2j}, t\right) = \sum_{\beta=1}^{N}\sum_{\alpha=1}^{M}\sum_{\gamma=1}^{L} B^{p}_{ij(x_{2j}-\alpha, y_{2j}-\beta, z_{2j}-\gamma)}\, \varepsilon^{p}_{ij(\alpha,\beta,\gamma)} \quad (7)$$

In equation (7), $B^{p}_{ij(x_{2j}-\alpha, y_{2j}-\beta, z_{2j}-\gamma)}$ is the influence coefficient of the plastic deformation of the rolling element and inner race. Both elastic deformation and plastic deformation are discrete according to the ICM method [16]. $\varepsilon^{p}_{ij(\alpha,\beta,\gamma)}$ is the equivalent plastic strain at the center of the small rectangular body.

Additionally, δ_1 and δ_2 in the film thickness equation replace the real surface roughness heights of the ball and the race.

In this study, the unified Reynolds equation is used to solve the pressure (including film pressure and asperity contact pressure) between the ball and the race are present by Zhu and Hu [17], as shown in Eq. (8). After solving the film thickness equation with elastoplastic deformation and real surface roughness, the obtained film thickness distribution will be taken into the Reynolds equation to find the required pressure by the finite difference method.

$$\frac{\partial}{\partial x_{2j}}\left(\frac{\rho h^3}{\eta}\frac{\partial p}{\partial x_{2j}}\right) + \frac{\partial}{\partial y_{2j}}\left(\frac{\rho h^3}{\eta}\frac{\partial p}{\partial y_{2j}}\right) = 12U\frac{\partial (ph)}{\partial x_{2j}} + 12\frac{\partial (ph)}{\partial t}. \quad (8)$$

The boundary conditions for solving Reynolds equation are as follows:

$$\begin{cases} p_{2j}|_{xin} = 0\ , p_{2j}|_{xout} = 0 \\ p_{2j}|_{yin} = 0\ , p_{2j}|_{yout} = 0 \\ p_{2j} = 0\left(if\ \ p_{2j} < 0\right) \end{cases} \quad (9)$$

When the thickness of the oil film is not enough to separate the rolling elements from the raceway, the rough peaks are in direct contact, and local stress is excessively concentrated under severe working conditions, causing the surface and subsurface stress to exceed the yield limit of the contact body. As a result, the internal structure of the matrix changes, and the pressure distribution on the contact surface changes accordingly.

Equations (10), (11), and (12) are all related to pressure distribution, so the equations in the following section are critical to the numerical calculation of the fatigue life of the three-dimensional elastoplastic hybrid lubrication.

As for the film viscosity[18]and the density[19], which are both related with film pressure and expressed as follows,

$$\eta = \eta_0 exp\{\ (ln\,\eta_0 + 9.67)\ \left[1 + 5.1 \times 10^{-9} p_{2j}\right]^{z} - 1\}. \quad (10)$$

$$\rho = \rho_0\left[1 + \frac{0.6\times10^{-9}p_{2j}}{1+1.7\times10^{-9}p_{2j}}\right]. \quad (11)$$

At last, by integrating the pressure considering elastoplastic deformation and real surface roughness, the total load can be obtained as,

$$\int\int p_{2j}(x_{2j}, y_{2j}, t)\, dxdy = w \quad (12)$$

2.3 Fatigue life model based on Elastoplastic mixed lubrication

In this study, based on the elastoplastic mixed lubrication analysis considering the real surface roughness and plastic deformation, a further bearing fatigue life model is established.

After getting the pressure on the surface by the analysis of 3D elastoplastic mixed

lubrication, the elastoplastic stress distribution below the surface can be solved by the DC-FFT method [20], and the calculation area is discretized to a spatial rectangular body as shown in Fig. 3. In the *x*, *y*, and *z* directions, the calculation area is divided into several equidistant rectangles with Δ_x, Δ_y, and Δ_z as the side lengths of the small rectangles. The stress distribution at the center point of each rectangular body can be solved, and then can be used as the calculation basis for the relative life and stress volume integral ratio.

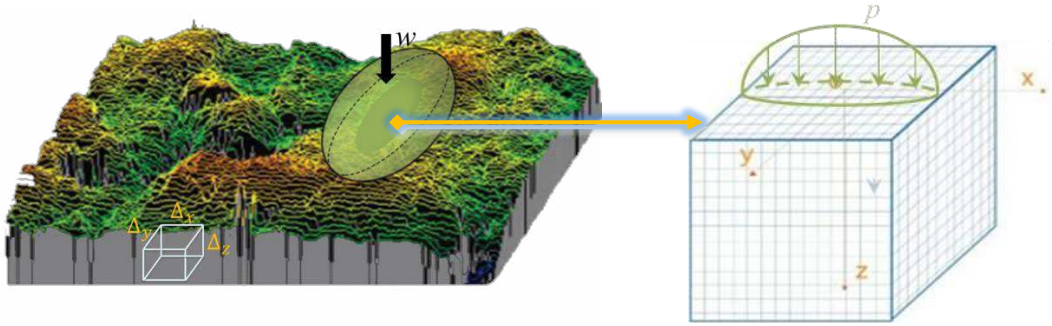

Fig. 2. Schematic of three-dimensional solution domain.

The formula for solving the stress of each center point is expressed as,

$$\sigma_{ij}(\alpha,\beta,\gamma) = c_{ij}^{\tau_{zz}}(\alpha,\beta,\gamma) + c_{ij}^{\tau_{zx}}(\alpha,\beta,\gamma) + c_{ij}^{\tau_{zy}}(\alpha,\beta,\gamma). \quad (13)$$

This study adopts a mathematical expression of the uniaxial stress-strain relationship, and the subsequent yield limit of the material can be expressed as follows,

$$\sigma_Y(\varepsilon^P) = \sigma_{Y0} + E_T/(1 - E_T/E)\varepsilon^P \quad (14)$$

Where E is the elastic modulus of the material, E_T is the tangent modulus, and σ_{Y0} is the initial yield limit. $ES = E_T/E$, where ES is the relative plastic modulus.

The life calculation uses the life prediction model established by Zaretsky [21]. As shown in equation (15), this model correlates the number of load cycles with the volume integral of the equivalent stress in the calculation domain [22-23] and discards the depth term and fatigue limit stress.

$$ln\frac{1}{S} \sim N^e \iiint_V (\sigma_{eq})^{e.c}\, dV \quad (15)$$

$$L_R = \left(\frac{\iiint_{V_0} \sigma_{eq}^{ec} dV}{\iiint_{V;} \sigma_{eq}^{ec} dV}\right)^{1/e} \quad (16)$$

$$\sigma_{vm} = \sqrt{[(\sigma_1 - \sigma_2)^2 + (\sigma_2 - \sigma_3)^2 + (\sigma_3 - \sigma_1)^2]/6} \quad (17)$$

Where σ_1, σ_2, and σ_3 are the first principal stress, the second principal stress, and the third principal stress, respectively.

$$\mathrm{Vol}(\sigma_{eq}) = \iiint_V \sigma_{eq}^{ec}\, dV \quad (18)$$

$$M_R = \frac{\iiint_{V;} \sigma_{eq}^{ec} dV}{\iiint_{V_0} \sigma_{eq}^{ec} dV} \quad (19)$$

Where S is the survival probability, N is the contact fatigue life (number of stress cycles), V is the stress volume, σ_{eq} is the equivalent stress (using von Mises stress), e is the Weibull slope, and c is the stress index. The relevant constants are taken as $S = 0.9$, $C = 9.1$, and $e = 10/9$ [24].

3. Numerical analysis method

Aiming at the prediction of the fatigue life of gas turbine bearings, firstly, based on the established three-dimensional elastoplastic

mixed lubrication model considering surface machined roughness and plastic deformation, the effects of working conditions, lubrication parameters, surface topography parameters, and material characteristic parameters on lubrication performance are studied. Further, the influences are further extended to the study on the fatigue life of the gas turbine bearing.

The model in this study can solve the drawbacks caused by only considering surface elastic deformation (i.e., generating pressure peaks many times higher than Hertzian pressure and subsurface stress fields far exceeding the yield limit of the material). The model can simulate cyclic loading bringing plasticity to gas turbine bearings as well as changes in material internal structure and resistance to deformation caused by accumulation of strain. This study considers both plastic deformation and real rough surface contact while investigating the fatigue life prediction of gas turbine bearings.

Figure 4 presents the calculation flowchart of the fatigue life considering elastoplastic mixed lubrication. Taking the measured rough surface and gas turbine bearing structure parameters, working condition parameters, and lubrication parameters as input data, the elastoplastic mixed lubrication equations are used to solve the subsurface stress field distribution. The von Mises yield criterion judges whether the resulting stress exceeds the yield limit of the contact body. When plastic yield occurs, the plastic strain is continuously iterated until the convergence accuracy is met. Then, the FFT method is used to obtain the residual stress and plastic deformation, and the plastic deformation generated by each calculation cycle is updated in real time on the surface topography of the gas turbine bearing. When the plastic deformation converges to obtain the stress distribution on the surface and subsurface of each node, the fatigue life is calculated according to the selected fatigue life model until the normal load reaches the preset value.

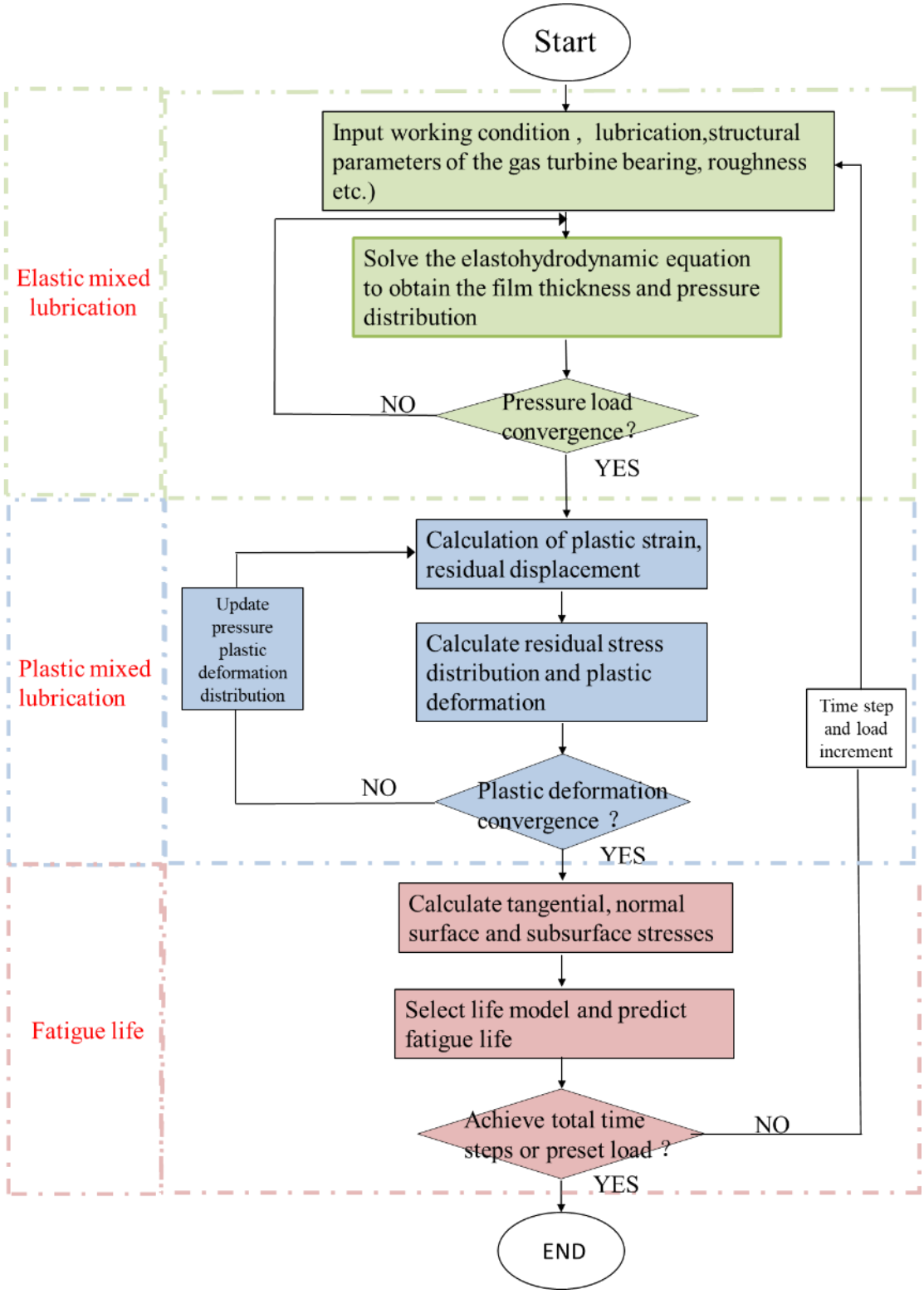

Fig. 4. Flowchart of calculation of relative life of gas turbine bearing elastoplastic hydrodynamic lubrication.

4. Results and discussions

4.1 Lubrication analysis result verification

The elastoplastic life prediction algorithm of the bearing is verified by comparing the stress field and film thickness distribution obtained by the SAM algorithm [25]. Table 1 lists the input parameters for the calculation. The contact body is assumed to be a rigid ellipsoid with ellipticity k = 2.0 on an infinitely extending elastoplastic plane, and 500 N normal load is applied to the rolling body, as shown in Fig. 5.

Figure 6 presents the main results of pressure peak, center oil film thickness, minimum oil film thickness, maximum residual stress, and maximum von Mises stress. It can be seen that the calculation results obtained by the method are highly consistent with the results obtained by the SAM method.

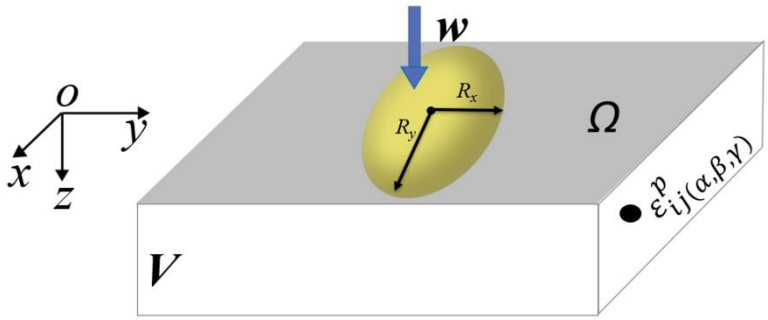

Fig. 5. Contact model of the calculation example.

Table 1. Input parameters of the calculation example.

Parameter	Unit	Ellipsoid	Flat
Applied load	N	500	
Radius of curvature in x direction R_x	mm	12.70	Infinity
Radius of curvature in y direction R_xR_y	mm	36.13	Infinity
Young's modulus	GPa	Rigid	206
Poisson's ratio		Rigid	0.3
Relative plastic modulus		Rigid	0.4
Initial yield limit	MPa	Rigid	500
Lubricant ambient viscosity	Pa·s	0.0262	
Pressure–viscosity coefficient	GPa^{-1}	12.5	

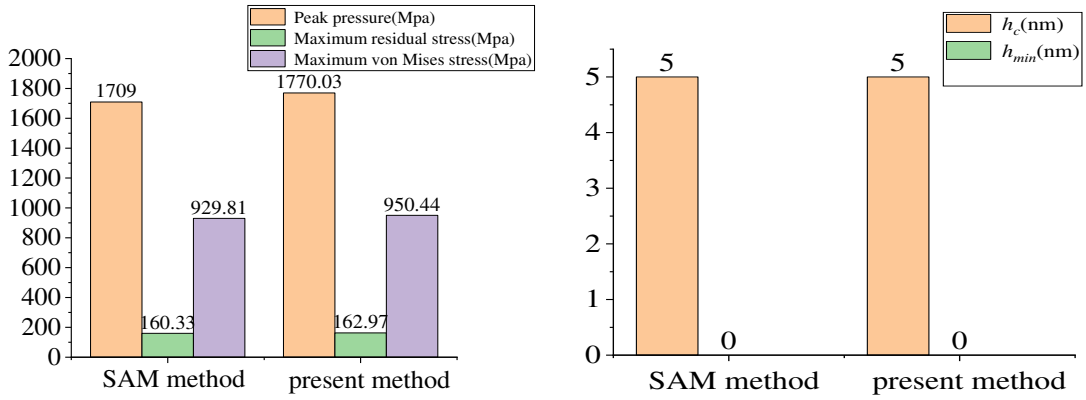

$U = 0.1$ m/s, (a) Stress distribution comparison, (b) Film thickness comparison

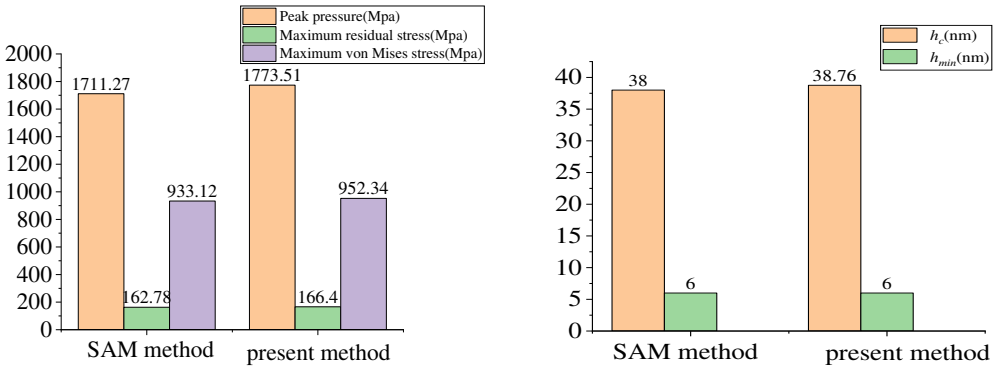

$U = 0.3$ m/s, (c) Stress distribution comparison, (d) Film thickness comparison

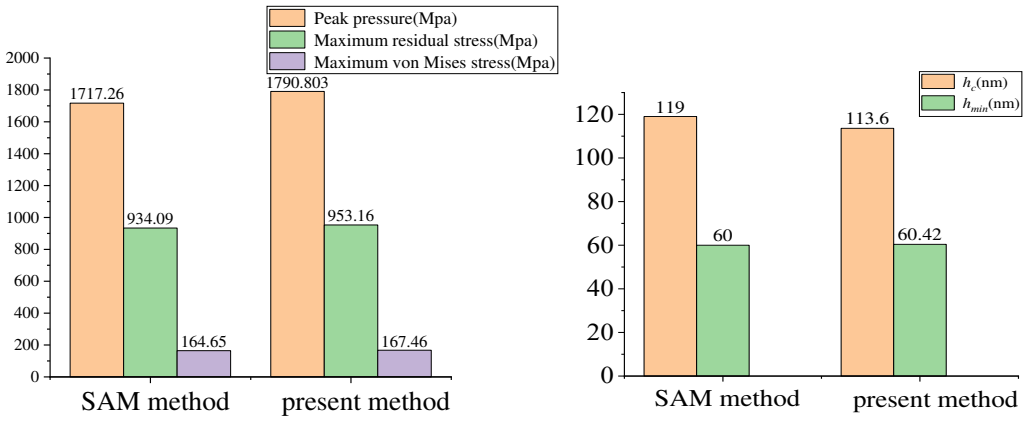

$U = 1$ m/s, (c) Stress distribution comparison, (d) Film thickness comparison

Fig. 6. Comparison diagram of results under different entrainment speeds.

4.2 The effect of material hardening characteristics on the fatigue life of gas turbine bearing

The calculation model in this paper is shown in Fig. 5. The relative plastic modulus of the elastic-plastic contact surface is adjusted to change the relative plastic modulus from 0 to 1 to study the influence of material properties on the relative life and the integral of the volumetric stress of the gas turbine bearing.

In the calculation, the load is 2000 N, the entrainment speed is 34.2 m/s, and the initial yield limit is 600 MPa.

The bearing and lubricant parameters are shown in Table 2. The relative plastic modulus $E_S = E/E_T$ is the ratio of the tangential modulus E_T to the equivalent elastic modulus E. In the calculation time, E_S is increased from 0 to 1 in increments of 0.2, with a total of six growth gradients. The dimensionless computational domain was chosen to be $2 \le X \le 2$, $-2 \le Y \le 2$, $0 \le Z \le 2$, and was divided into a 128×128×40 grids in the X, Y and Z direction, respectively.

Table 2. Gas turbine bearing and lubricant parameters.

Parameter	Value
Bearing inner diameter	220 mm
Ball diameter	47.625 mm
Initial contact angle	26°
Curvature coefficient of inner/outer channel	0.515/0.515
Density	885 ρ/ kg·m3
Lubricant ambient viscosity	0.0262 Pa·s
Pressure–viscosity coefficient	1.25×10^{-8} Pa^{-1}

Figure 7 shows the CBN grinding surface used in the calculation, and the roughness values of R_a, R_q, and R_t are given. Figure 8 plots the results of the stress volume integral ratio and relative fatigue life of the smooth surface and the rough surface under different hardening levels. It can be seen that during the transition from pure plasticity to pure elasticity on the contact surface and subface, the stress volume integral ratio gradually increases while the relative life expectancy decreases.

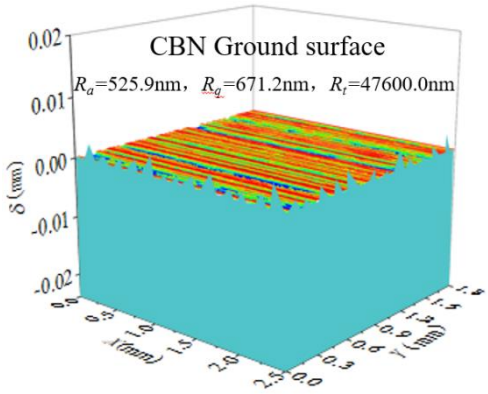

Fig. 7. The real rough surface used in the calculation.

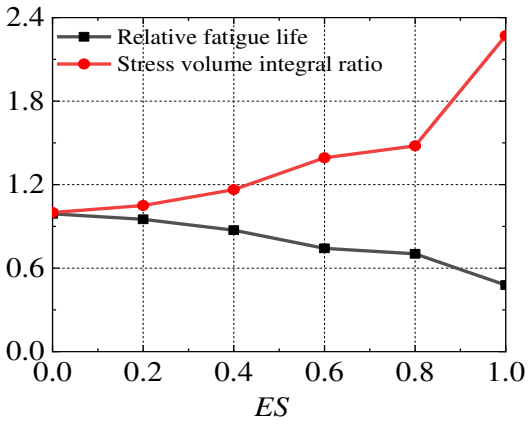

Fig. 8. Influence of material hardening properties on relative fatigue life

Figure 9 shows the change in the stress volume integral ratio of the elastoplastic material and the pure elastic material with smooth and real rough surfaces. As shown, the pure elastic stress volume integral of rough and smooth surfaces is much higher than those of elastoplastic stress, and due to the presence of rough peaks, local surface and subsurface stress concentration causes the stress volume integral of a rough surface to be greater than that of a smooth surface. Since the purely elastic surface is not restricted by the initial yield limit of the material, it is more likely to cause stress concentration to produce a larger stress peak.

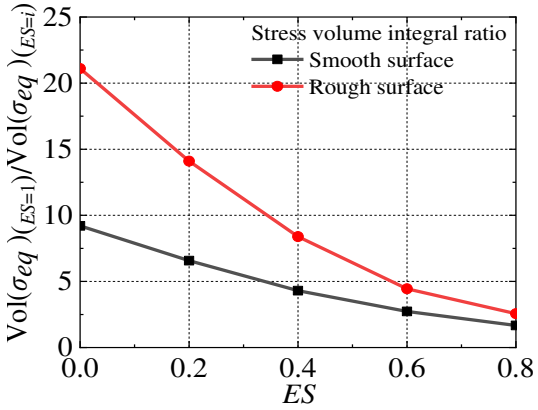

Fig. 9. Effect of material hardening properties on stress volume integral ratio

Figures 10 and 11 depict the surface and surface stress distribution when the hardening grade is 0.4 and 0.8, respectively, which show that the increased elasticity of the material and the contact of the real rough peaks will cause the surface and subsurface stress to rise, and plastic deformation within a reasonable range can reduce the contact stress and extend the relative fatigue life of the bearing.

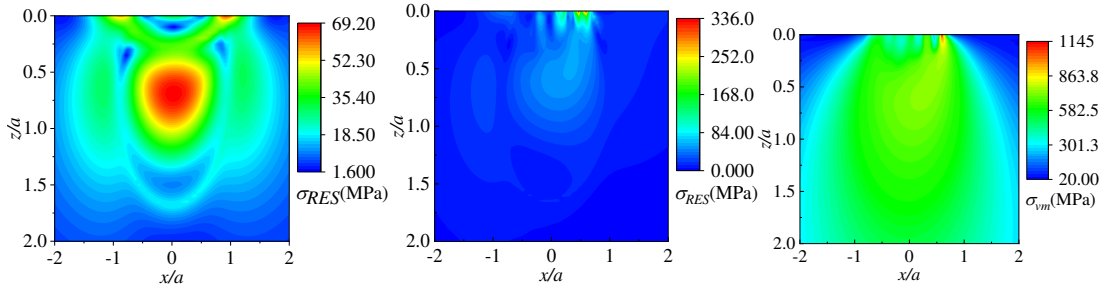

(a) Smooth solution of residual stress. (b) Rough solution of residual stress. (c) Rough solution of

von Mises stress.

Fig. 10. Residual stress and three-dimensional cloud diagrams of smooth and rough von Mises stress when relative plastic modulus is 0.4.

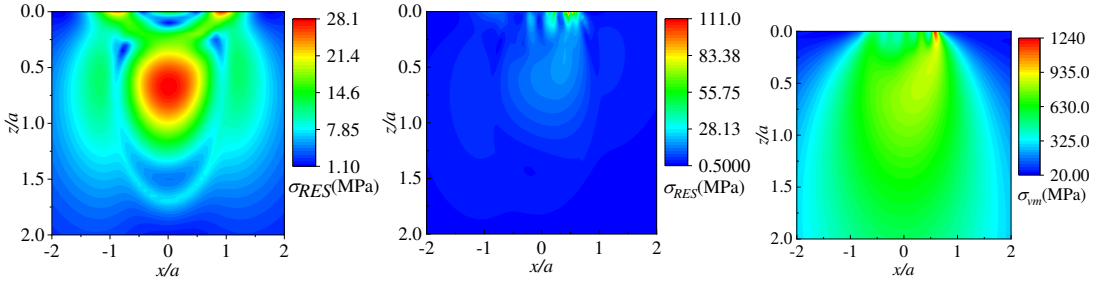

(a) Smooth solution of residual stress.(b) Rough solution of residual stress. (c) Rough solution of von Mises stress.

Fig. 11. Residual stress and three-dimensional cloud diagrams of smooth and rough von Mises stress when relative plastic modulus is 0.8.

4.3 The influence of load on fatigue life of gas turbine bearing

Heavy load is one of the important causes of plastic deformation. Excessive load is likely to produce contact stress exceeding the yield limit of the bearing material itself, causing excessive concentration of surface and subsurface contact stress in the local contact area between the rolling element and the raceway, and thereby shortening the service life of the gas turbine bearing. Hence, it is necessary to study the influence of load on the lubrication performance and relative fatigue life under the condition of elastoplastic mixed lubrication with the real rough surface.

In this study, two calculation examples are selected for comparison, namely, elastic relative fatigue life, elastoplastic relative fatigue life. In the three calculation examples, the required working condition parameters, structural parameters, lubricating oil parameters, and calculation domain are the same as those in section 4.2. Carry out the research work on the load conditions of 500N-3000N, and with 500N as the increasing gradient to increase the relative fatigue life of gas turbine bearings.

Fig. 12 plots the dimensionless plastic deformation of the elastoplastic mixed lubrication contact area with the real rough surface, where the positive numerical solution of plastic deformation means that the position has a concave deformation, and vice versa.

Figure 13(a) and (b) respectively plot the elastoplastic relative fatigue life, stress volume integral ratio and three-dimensional oil film pressure contours of the gas turbine bearing. It can be seen that the relative fatigue life show different trends, for $E_S = 1$, namely pure elastic case, when the load increased from 500 N to 3000 N, the stress volume integral ratio increased by 126%, and the relative life was reduced by 52%. However, for $E_S = 0.4$, namely considering the influence of the plastic deformation, the stress volume integral ratio only increase by 48.6%, and the relative life was reduced by 43.2%, the magnitude change was relatively more gentle. According to Fig. 12 and Fig. 13, it can be seen that the presence of plastic deformation reduces the elastoplastic high-pressure area and the peak pressure.

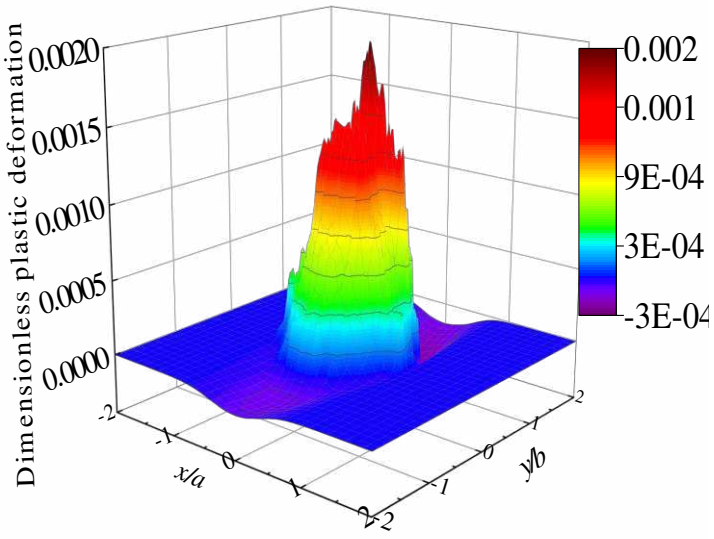

Fig. 12. Dimensionless plastic deformation, w = 2000 N.

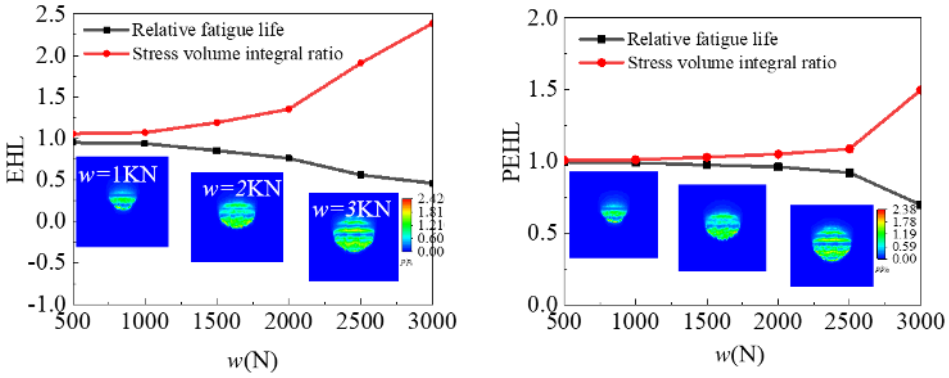

(a) for E_S = 1 (b) for E_S = 0.4.

Fig. 13. The influence of loads on the elastoplastic relative fatigue life solution of gas turbine bearing

4.4 The influence of machined roughness on the fatigue life of the gas turbine bearing

Considering the influence of real roughness on the relative fatigue life of gas turbine bearings under the condition of elastoplastic mixed lubrication, the initial yield limit of the contact material is 600 MPa, the effect of elastoplastic lubrication and relative fatigue life with smooth surface and R_q = 0.1 μm, R_q = 0.3 μm, R_q = 0.5 μm are compared. The Hertzian contact radius corresponding to a normal load of 1500 N is 0.23 mm, b is 2.5 mm, and the maximum Hertzian contact pressure is 1.61 GPa.

Figure 14 is a comparison of the pressure and film thickness in the contact zone with different roughness under elastoplastic mixed lubrication conditions. During the calculation process, the root mean square deviation of the surface profile takes the same value for the rolling element and the inner raceway. It can be found that the real surface roughness causes the gas turbine bearing contact pressure and film thickness to fluctuate irregularly around the smooth solution. As the real surface roughness increases, the amplitude of the fluctuation increases, and at the same time, greater contact pressure is generated. This is due to the

irregularity of the actual roughness, which will cause greater depression or protrusion deformation on the contact surface. At the place marked in the figure, due to the existence of plastic deformation, the uncontacted low roughness peaks come into contact, resulting in a new pressure peak.

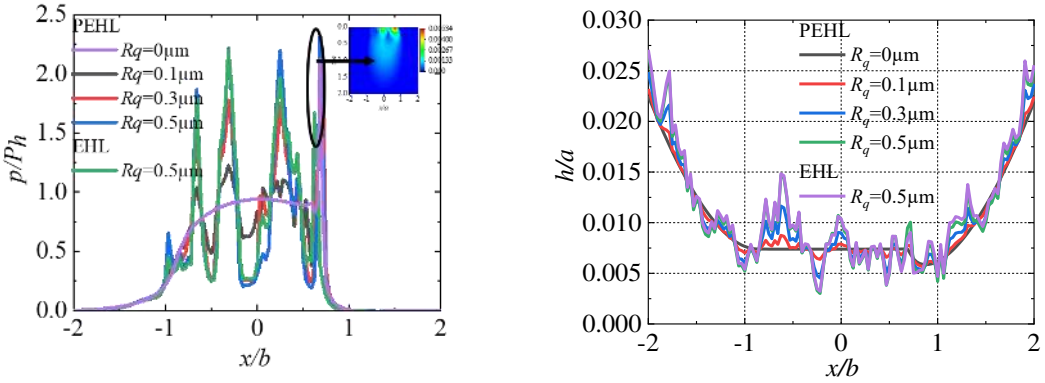

(a) Pressure comparison (b) Film thickness comparison

Fig. 14. Influence of roughness on film thickness and pressure of the gas turbine bearing

Figure 15 shows the residual stress distribution on the lower surface of the bearing. It can be seen that the uneven texture of the material surface will cause local stress concentration, resulting in uneven plastic deformation, which is the main cause of residual stress. Appropriate distribution of residual stress is helpful to maintain the internal structure balance, otherwise it will cause deformation, cracking and other accidents.

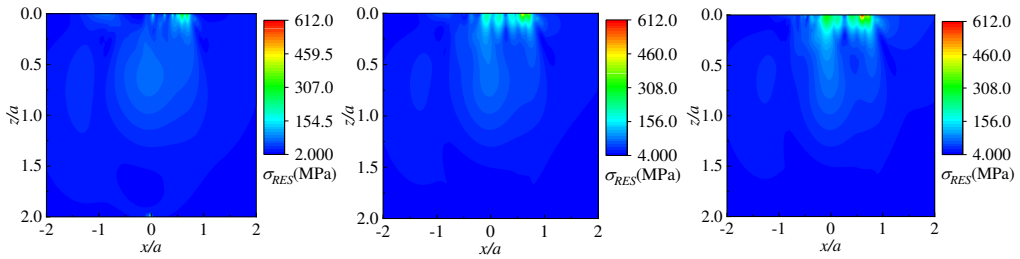

(a) $R_q = 0.1$ μm (b) $R_q = 0.3$ μm (c) $R_q = 0.5$ μm

Fig. 15. The effect of the real roughness on the residual stress distribution of the gas turbine bearing

In Fig. 16(a) and (b), the relative fatigue life and stress volume integral ratio of PEHL and EHL are plotted. The relative fatigue life of PEHL is slightly longer than that of EHL under the same working conditions. This is due to the lack of the relative considerations of the material hardness and the material characteristics under EHL conditions, which would obtain the inaccurate surface and subsurface stresses in the process of relative life calculation.

As shown, the relative fatigue life is greater when the roughness is smaller. The relative life of PEHL is longer when R_q = 0.1 μm, and the EHL one is increased by 26.3%, and the gap between the two gradually increased as the true roughness increased. Under the same R_q values, the EHL stress volume fraction ratio was much larger than those in PEHL conditions. It can be seen that the increase in true roughness would cause the surface and subsurface stress to become

concentrated, resulting in a larger stress peak, which is not conducive to the service life of the gas turbine bearing.

At the same time, the presence of plastic deformation helps to reduce the surface and subsurface stress distribution, and the reduction effect is positively related to the amount of plastic deformation. It can be seen that proper plastic deformation can reduce contact stress and prolong fatigue life without causing damage to the gas turbine bearing structure.

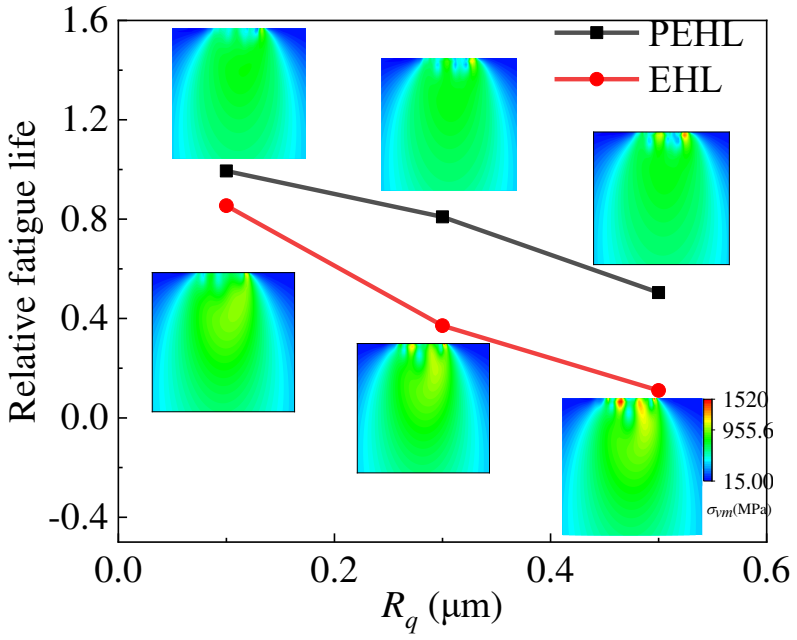

(a) Comparison of relative life

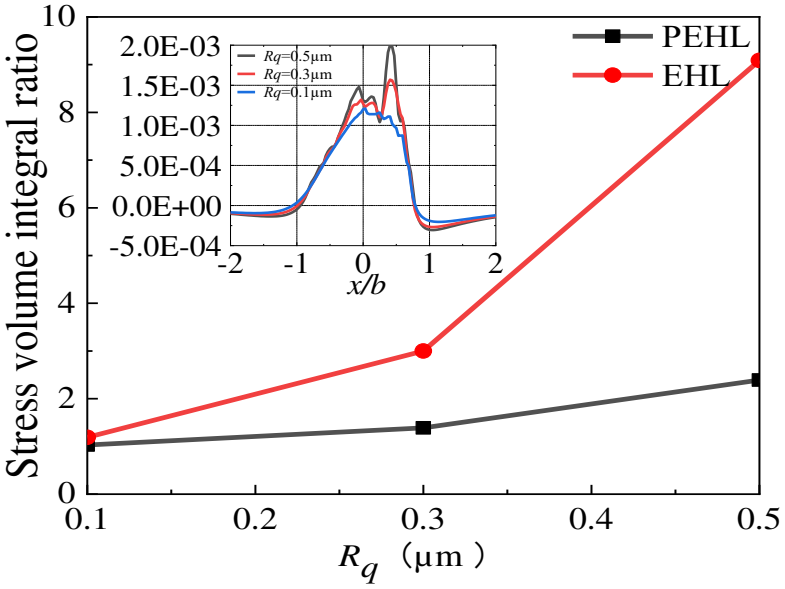

(b) Comparison of stress volume integral

Fig. 16. Comparison of relative life and stress volume integral of PEHL and EHL under different roughness values

5. Conclusions

Based on the typical working conditions of gas turbine bearings, and considering the effects of real rough surface and plastic deformation, a 3D elastoplastic mixed lubrication model is established to predict the relative fatigue life, and the effects of material hardening, load, and real roughness on the relative life are investigated. The findings are summarized as follows:

(1) By comparing the fatigue life of elastic mixed lubrication and elastic-plastic mixed lubrication, the fatigue life value of elastic mixed lubrication is lower, due to the lack of material initial yield limit, it is easier to cause surface and subsurface stress concentration.

(2) When the material relative plastic modulus of bearing and inner ring is 0.4, the relative fatigue life is in the most favorable condition. If the plastic property is too strong, it is easy to generate stress in deeper layer, and the area is larger. Whereas, when the elastic property is too strong, it will produce higher surface and subsurface stress peaks. Both of them are unfavorable to the service life of bearing.

(3) Compared with PEHL solution and EHL solution, the existence of plastic deformation reduces the area and maximum peak value of the surface pressure under heavy load condition. Furthermore, it has been proved that plastic deformation may be allowed to change in an appropriate range in practical engineering in order to prolong the service life of bearing.

(4) The increase of real surface roughness is likely to cause the increase of surface pit or bulge deformation, and then affect the distribution of pressure and film thickness, next resulting in the concentration of surface stress, which will finally reduce the fatigue life of bearing. In a word with the increase of roughness, the decrease in EHL fatigue life is more obvious.

References

[1] Wang L.Q., Design and numerical analysis of rolling element bearing for extreme applications. Harbin: Harbin Institute of Technology Press, 2013.

[2] Chen G.C., Thermal analysis of high-speed rolling bearing used in main-shaft of aero-engine (Ph.D. thesis). Harbin: Harbin Institute of Technology, 2008.

[3] Akamatsu Y., Tsushima N., Goto T., Hibi K., Influence of surface roughness skewness on rolling contact fatigue life. Tribology Transactions, 1992. **35**(4): 745-750.

[4] Zhai X., Chang L., Hoeprich M., Nixon H.P., On mechanisms of fatigue life enhancement by surface dents in heavily loaded rolling line contacts. Tribology Transactions, 1997. **40**(4): 708-714.

[5] Zhu D., Ren N., Wang Q.J., Pitting life prediction based on a 3D line contact mixed EHL analysis and subsurface von Mises stress calculation. Journal of Tribology, 2009. **131**(4): 041-501.

[6] Yan X.L., Wang X.L., Zhang Y.Y., A parametric study on fatigue life for mixed elastohydrodynamic lubrication point contacts. Journal of Tribology, 2013. **135**(4): 041-501.

[7] Yan X.L., Wang X.L., Zhang Y.Y., Influence of roughness parameters skewness and kurtosis on fatigue life under mixed elastohydrodynamic lubrication point contacts. Journal of Tribology, 2014. **136**(3): 031-503.

[8] Lu Y.D., analysis of lubrication performances for rolling bearing based on real rough surface. Taiyuan: Taiyuan University of Science and Technology, 2016. 1-70.

[9] Oswald F.B., Zaretsky E.Y., Poplawski J.V., Relation between residual and hoop stresses and rolling bearing fatigue life. Tribology Transactions, 2014. **57**(3): 749-765.

[10] Li D.L., Study on 3D elasto-plastic rolling/sliding contact problems, Chongqing: Chongqing University, 2015. 45-71.

[11] Xie L., Palmer D., Otto F., et al., Effect of surface hardening technique and case depth on rolling contact fatigue behavior of alloy steels. Tribology Transactions, 2014. **58**(2): 215-224.

[12] Pu C., Du M.G., Meng F.M., Analysis of elastoplastic contact performances for deep groove ball bearing considering roughness. Journal of Chongqing University, 2017. **40**(10): 12-22.

[13] Pu C., Study on elastohydrodynamic lubrication and noise of grease-lubricated deep groove ball bearings, Chongqing: Chongqing University, 2018. pp.26-30

[14] Lu X., Low cycle fatigue life of space bearings based on elastoplastic damage constitutive model, Henan: Henan University of Science and Technology, 2017. pp.45-54

[15] Harati E., Karlsson L., Svensson L.E., et al. The relative effects of residual stresses and weld toe geometry on fatigue life of weldments. International Journal of Fatigue, 2015, **77**: 160-165.

[16] Wang Z.J., Jin X.Q., Keer L.M., Wang Q., Novel model for partial-slip contact involving a material with inhomogeneity. Journal of Tribology, 2013. **135**(4): 041-401.

[17] Hu Y.Z., Zhu D., A full numerical solution to the mixed lubrication in point contacts. Journal of Tribology, 2000. **122**(1): 1-9.

[18] Roelands C.J.A., Correlation aspects of viscosity-temperature-pressure relationship of lubricating oils PhD Thesis Netherlands. Delft University of Technology, 1966.

[19] Dowson D., Higginson G.R., Elastohydrodynamic lubrication. New York: Pergamon Press, 1977.

[20] Liu S., Wang Q., Liu G., A versatile method of discrete convolution and FFT (DC-FFT) for contact analyses. Wear, 2000. **243**(1): 101-111.

[21] Zaretsky E.Y., Fatigue criterion to system design life and reliability. Journal of Propulsion and Power, 1987. **3**(1): 76-83.

[22] Zhou Q.H., Jin X.Q., et al., Numerical EIM with 3D FFT for the contact with a smooth or rough surface involving complicated and distributed inhomogeneities. Tribology International, 2016. **93**: 91-103.

[23] Shi X.J., Wang L.Q., Qin F.， Relative fatigue life prediction of high-speed and heavy-load ball bearing based on surface texture. Tribology International, 2016. **101**:

p. 364-374.

[24] Akamatsu Y., Tsushima N., Goto T., Hibi K., Influence of surface roughness skewness on rolling contact fatigue life. Tribology Transactions, 1992. **35**(4): 745-750.

[25] Jacq C., Nelias D., Lormand G., Girodin D., Development of a three-dimensional semi-analytical elastic-plastic contact code. Journal of Tribology, 2002. **124**(4): 653-667.

Figures

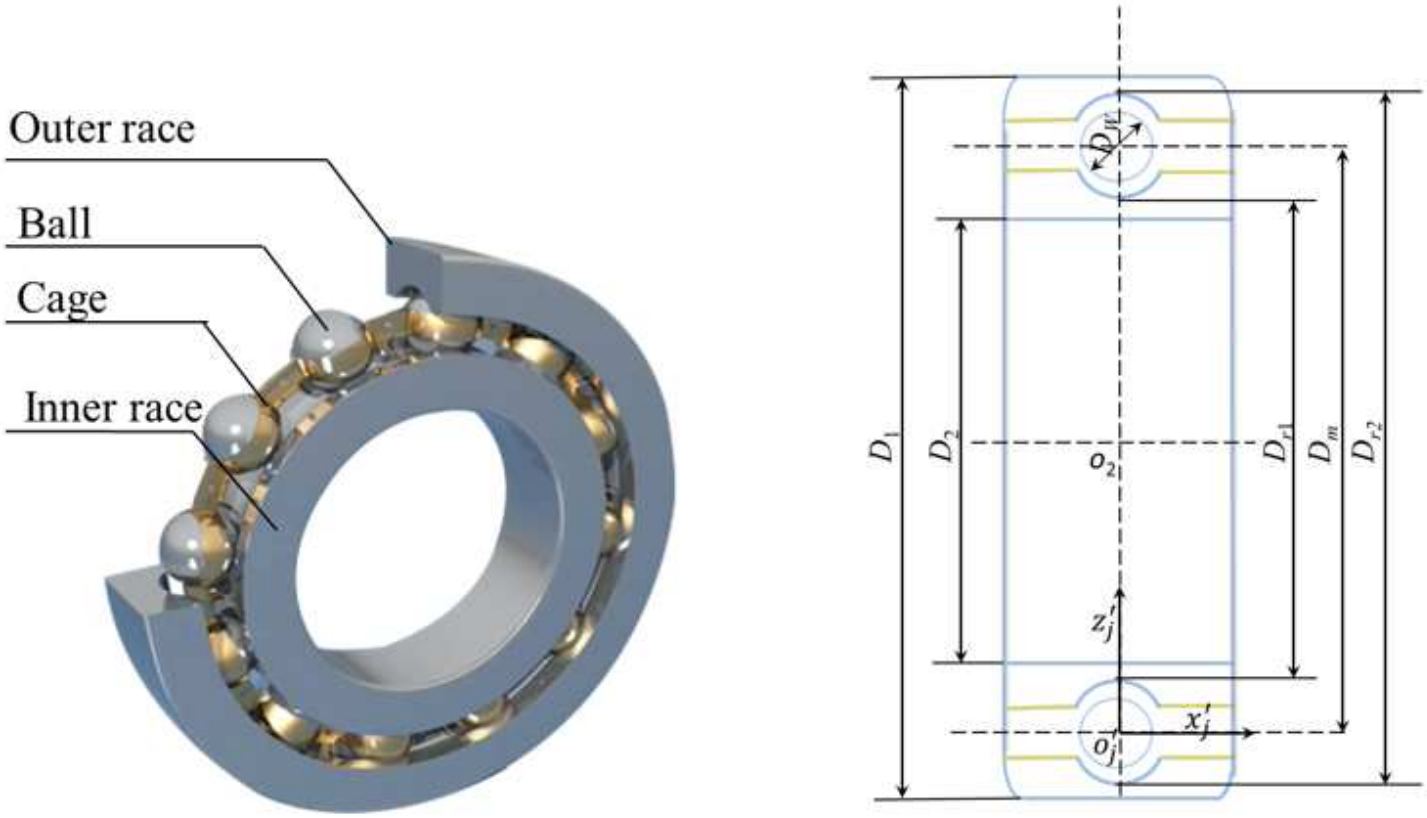

Figure 1

Gas turbine and gas turbine bearing plan.

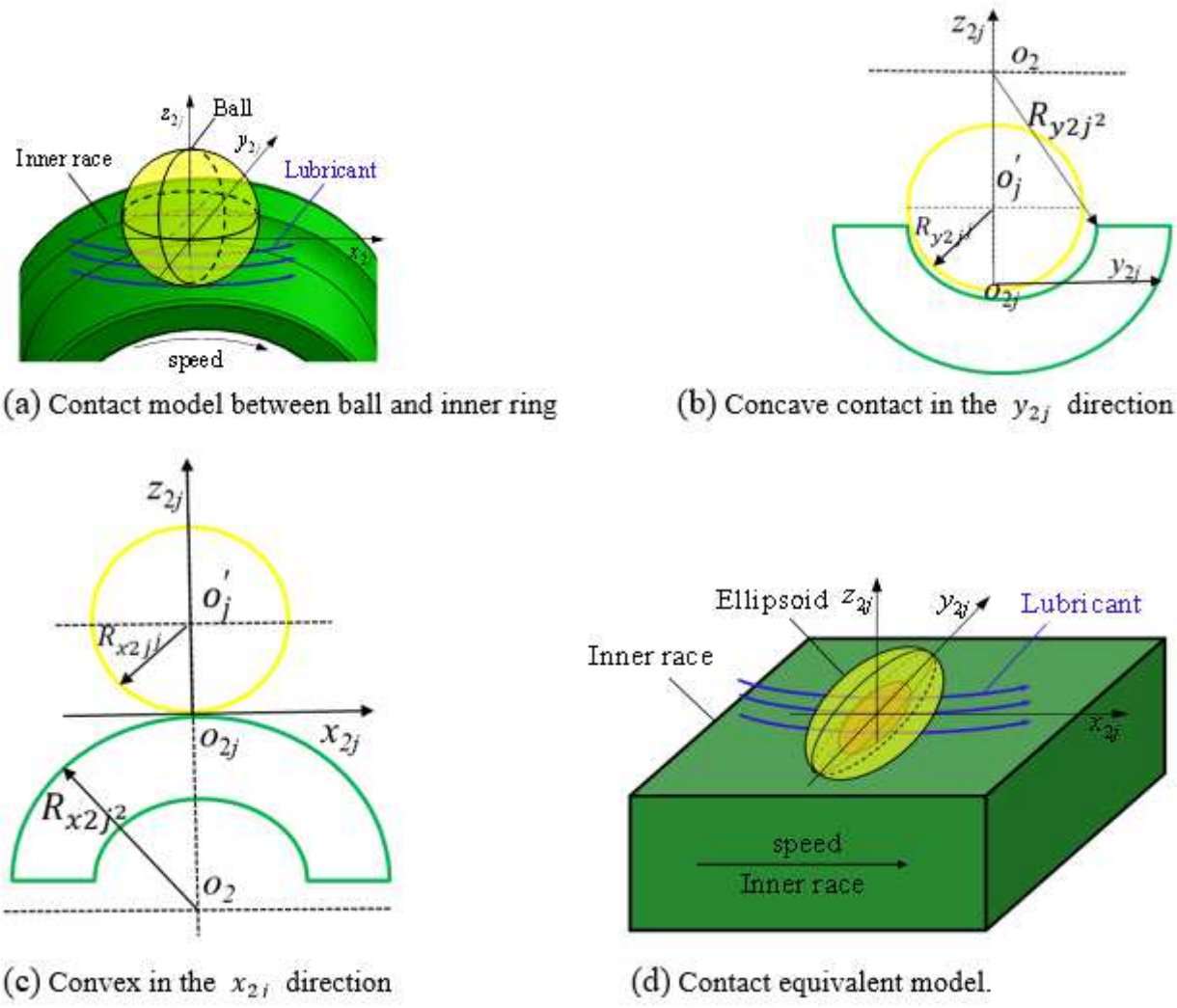

Figure 2

Contact equivalent diagram of rolling element and inner ring.

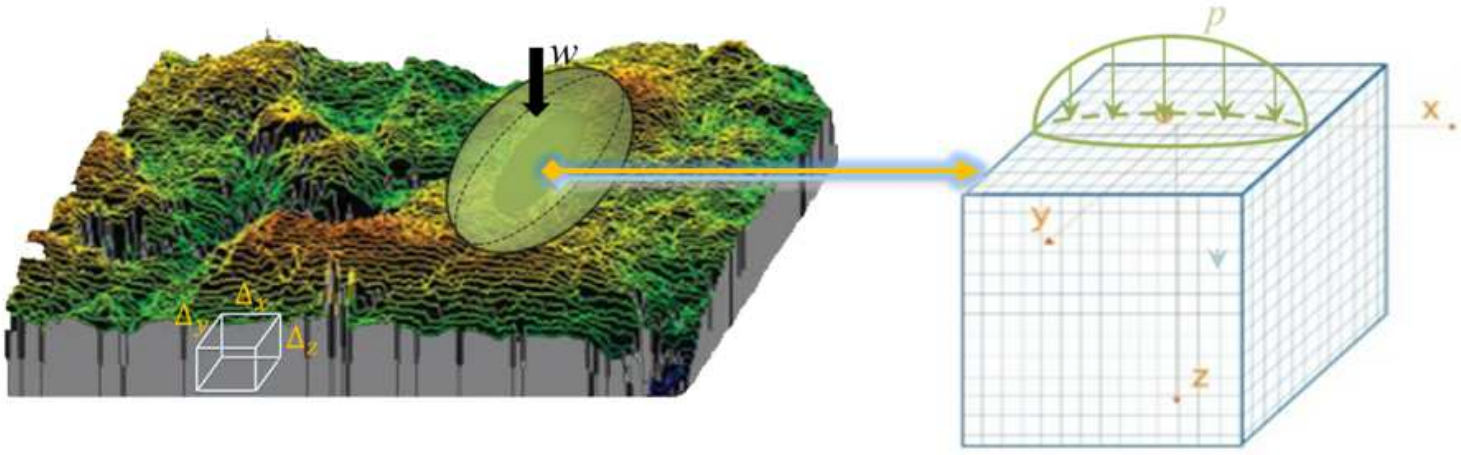

Figure 3

Schematic of three-dimensional solution domain.

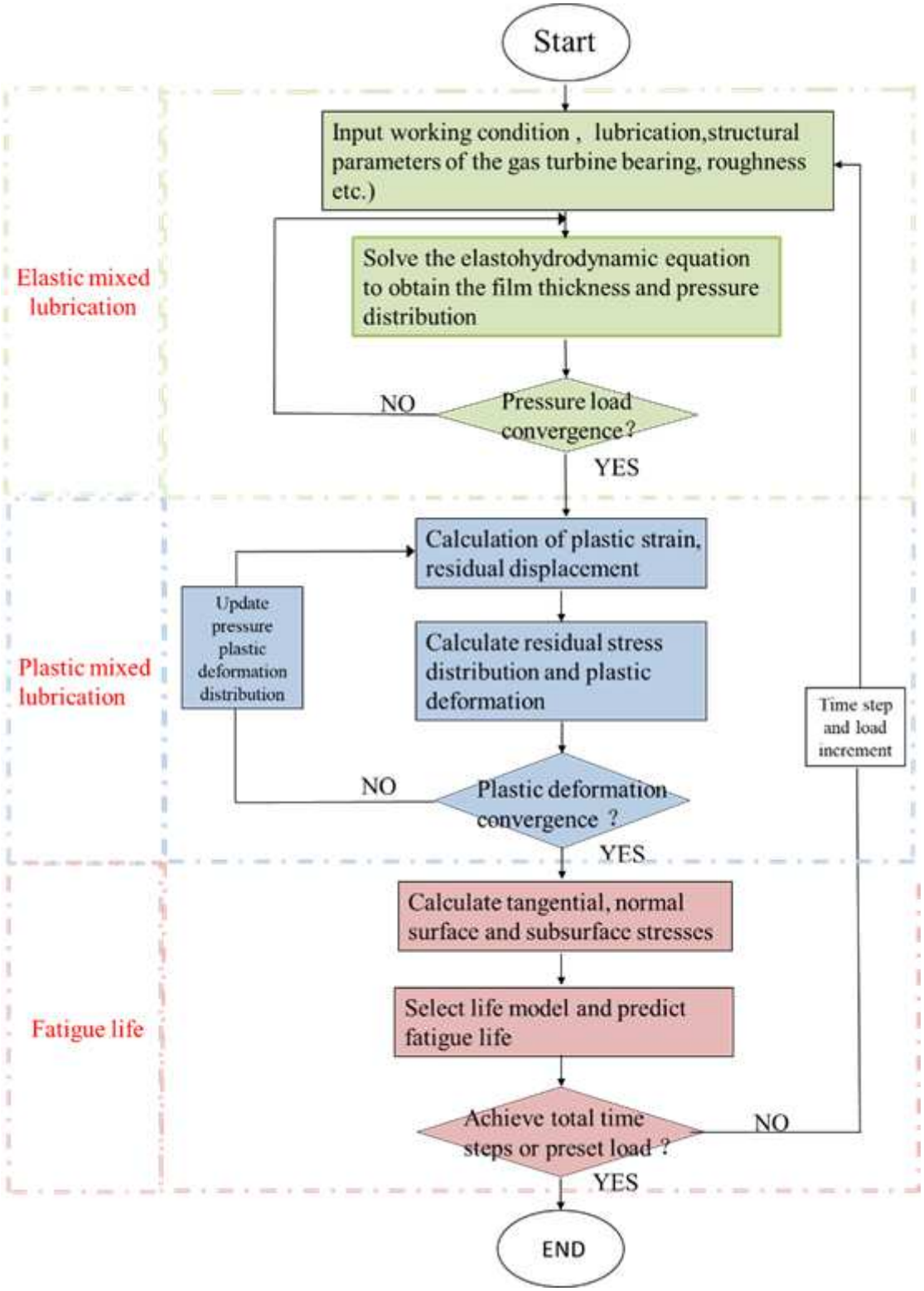

Figure 4

Flowchart of calculation of relative life of gas turbine bearing elastoplastic hydrodynamic lubrication.

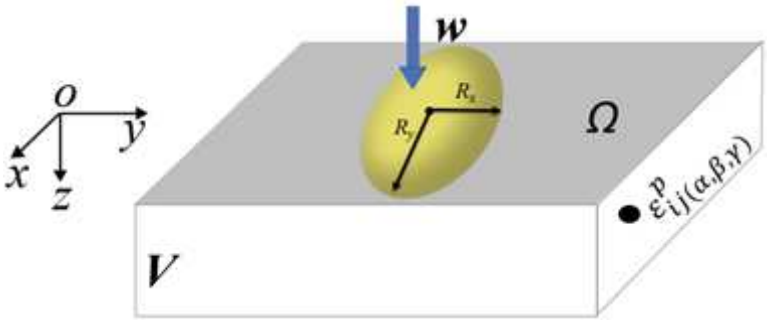

Figure 5

Contact model of the calculation example.

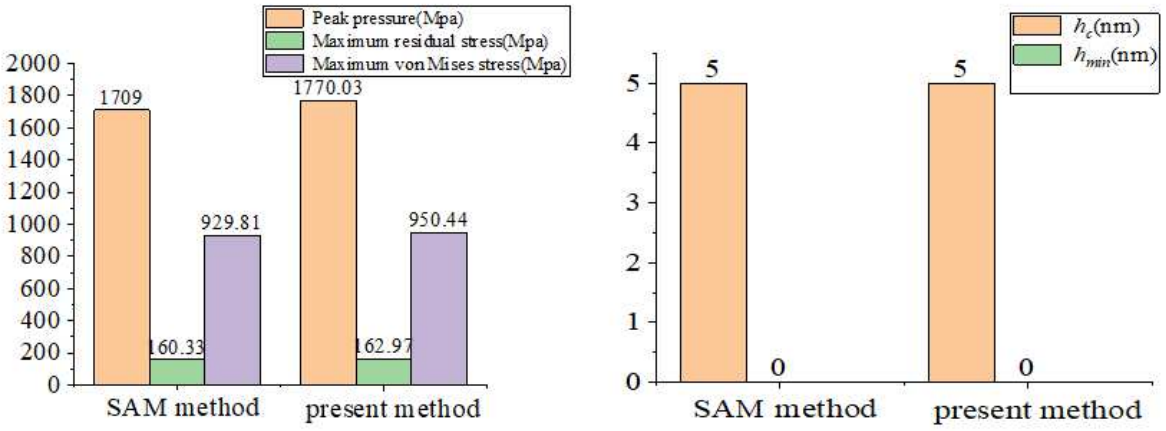

$U = 0.1$ m/s, (a) Stress distribution comparison, (b) Film thickness comparison

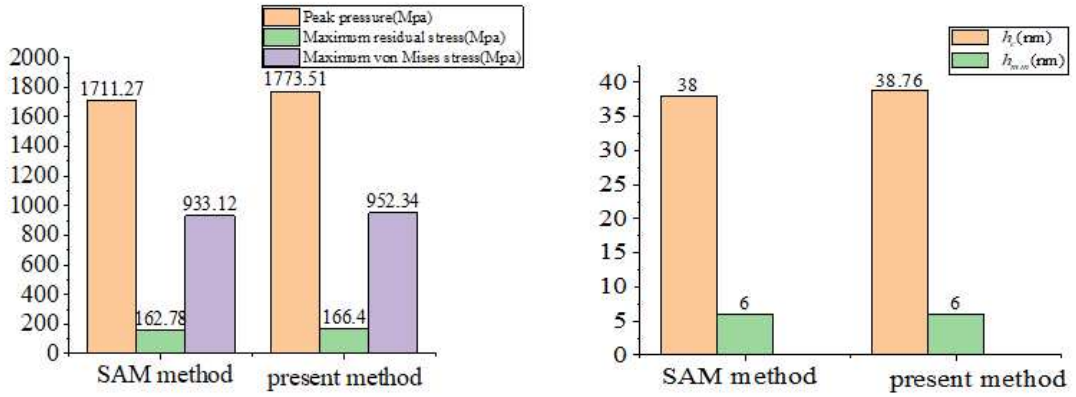

$U = 0.3$ m/s, (c) Stress distribution comparison, (d) Film thickness comparison

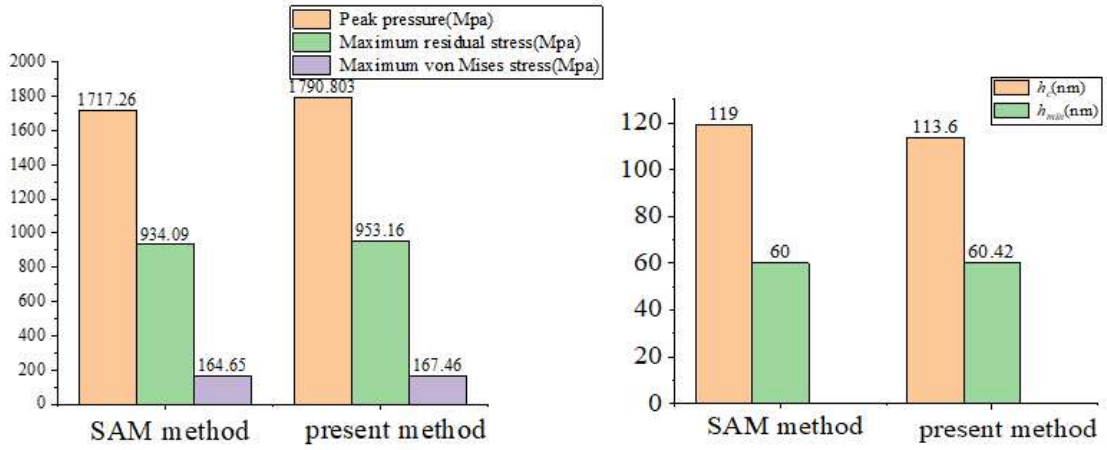

$U = 1$ m/s, (c) Stress distribution comparison, (d) Film thickness comparison

Figure 6

Comparison diagram of results under different entrainment speeds.

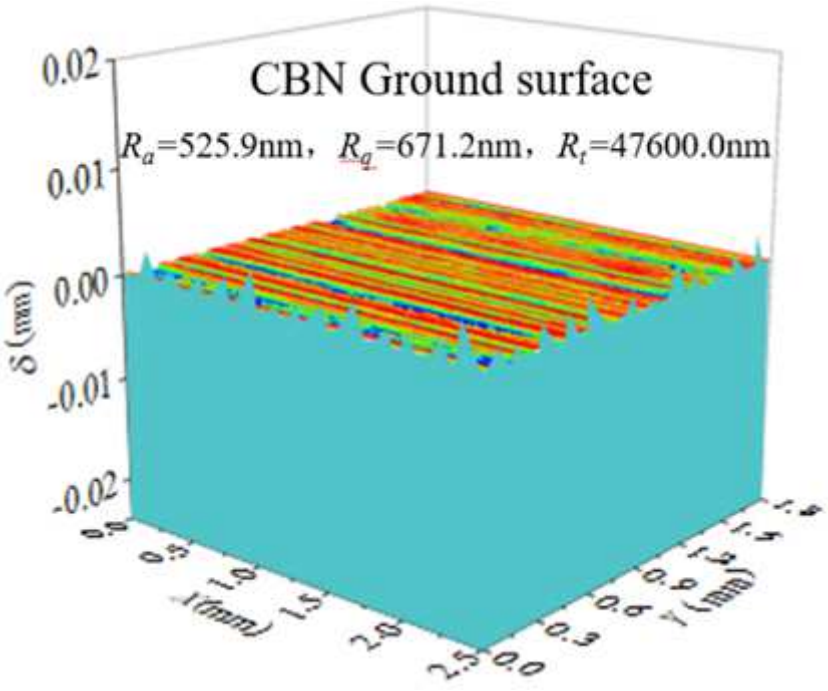

Figure 7

The real rough surface used in the calculation.

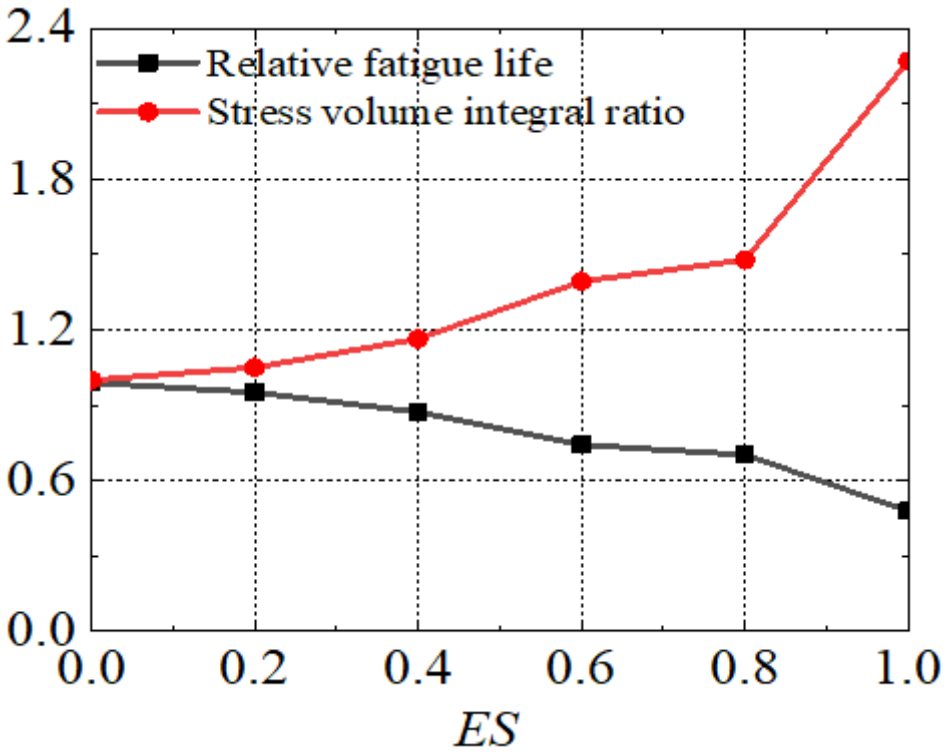

Figure 8

Influence of material hardening properties on relative fatigue life

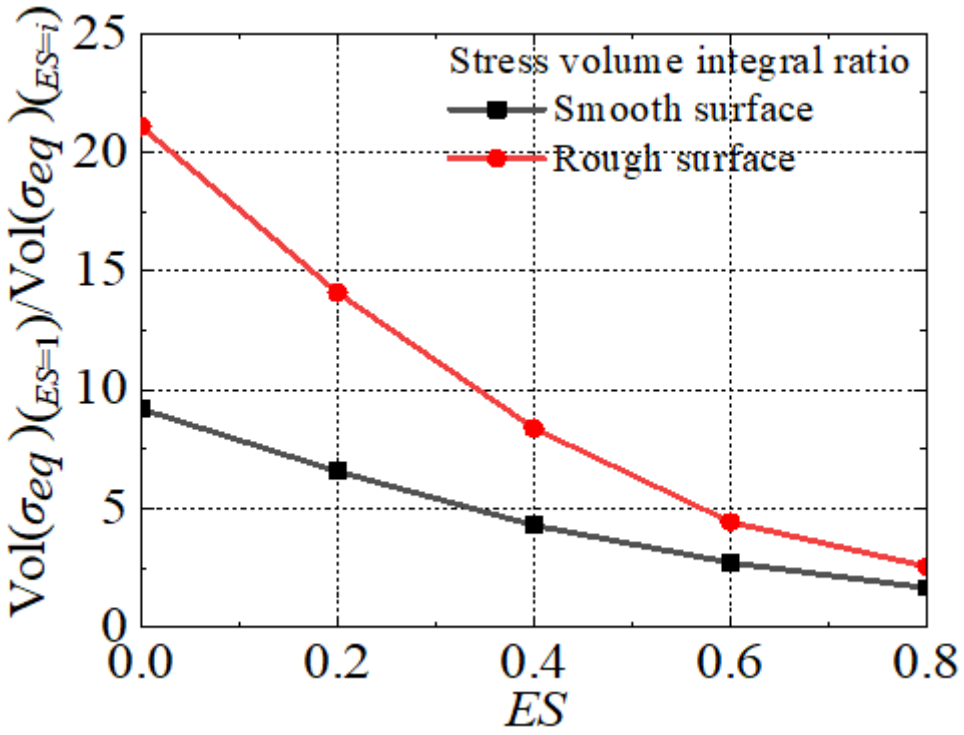

Figure 9

Effect of material hardening properties on stress volume integral ratio

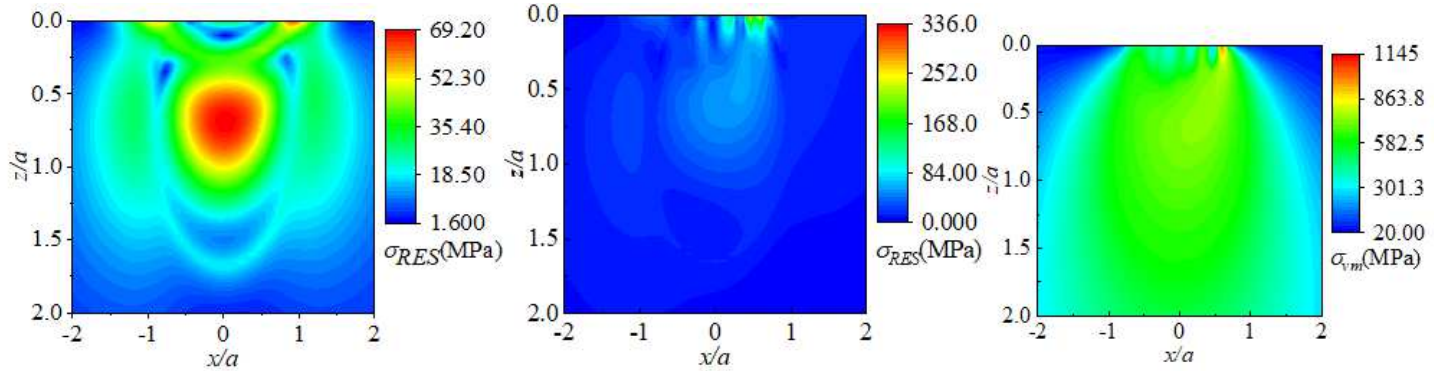

(a) Smooth solution of residual stress. (b) Rough solution of residual stress. (c) Rough solution of von Mises stress.

Figure 10

Residual stress and three-dimensional cloud diagrams of smooth and rough von Mises stress when relative plastic modulus is 0.4.

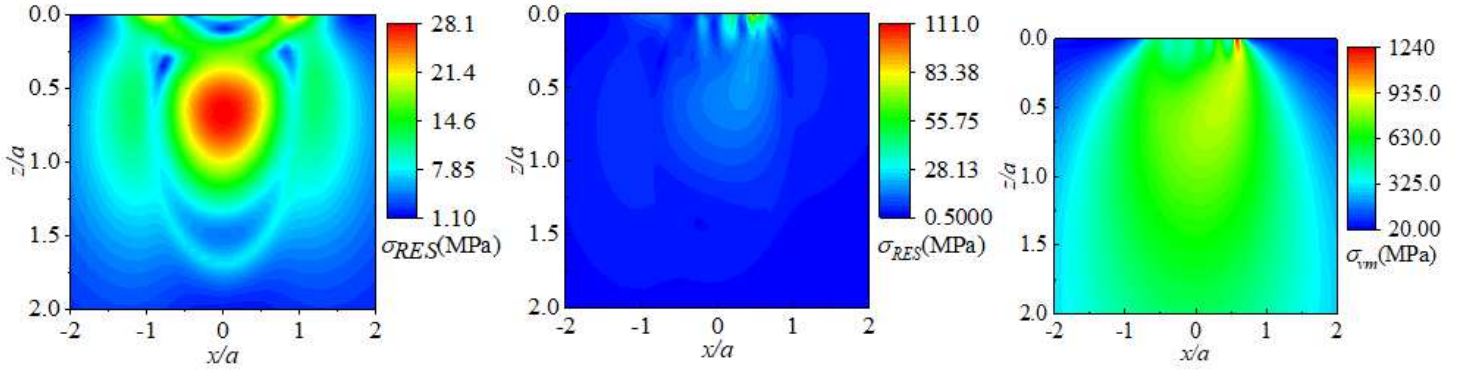

(a) Smooth solution of residual stress.(b) Rough solution of residual stress. (c) Rough solution of von Mises stress.

Figure 11

Residual stress and three-dimensional cloud diagrams of smooth and rough von Mises stress when relative plastic modulus is 0.8.

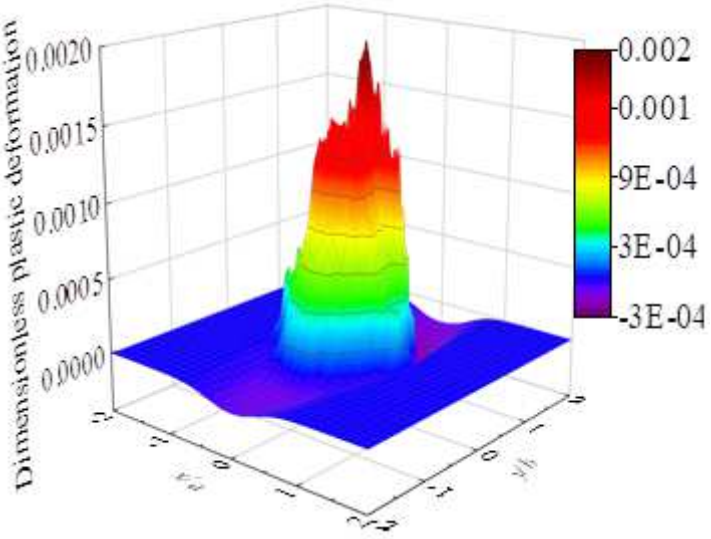

Figure 12

Dimensionless plastic deformation, w = 2000 N.

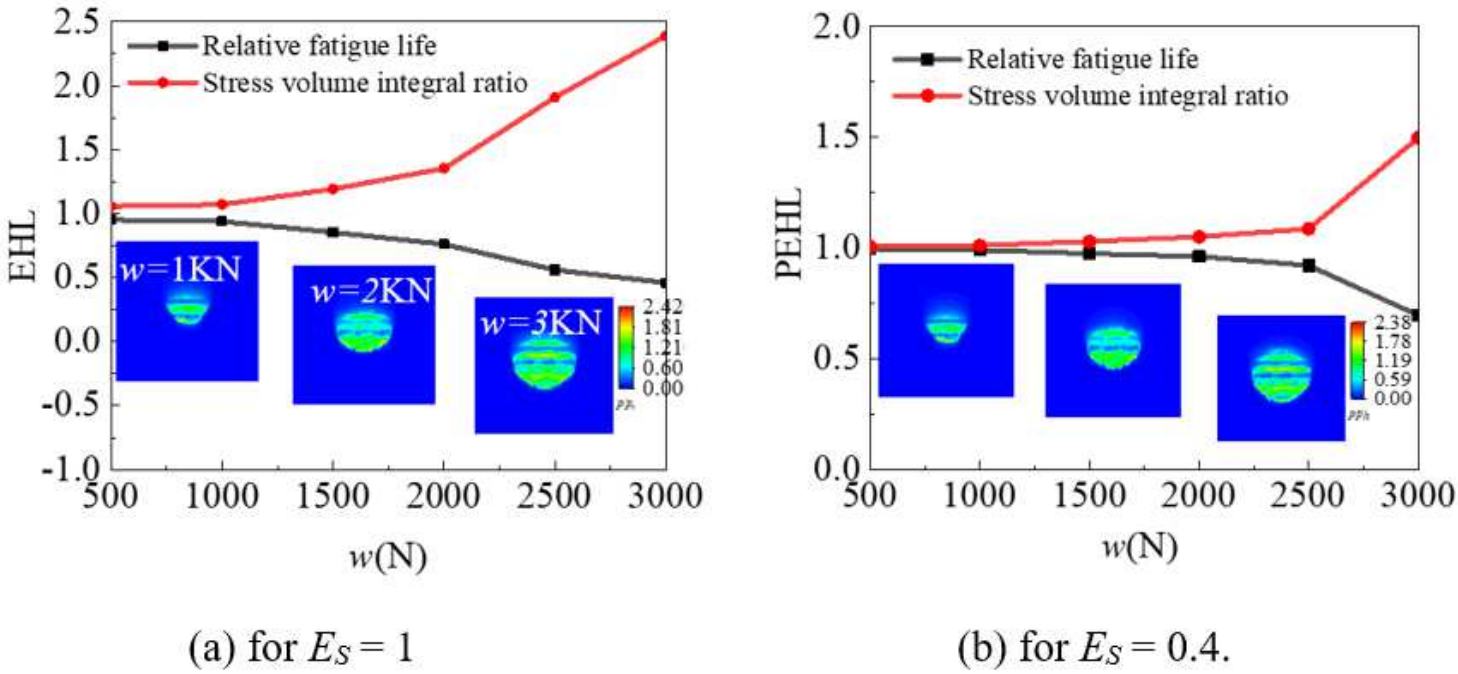

Figure 13

The influence of loads on the elastoplastic relative fatigue life solution of gas turbine bearing

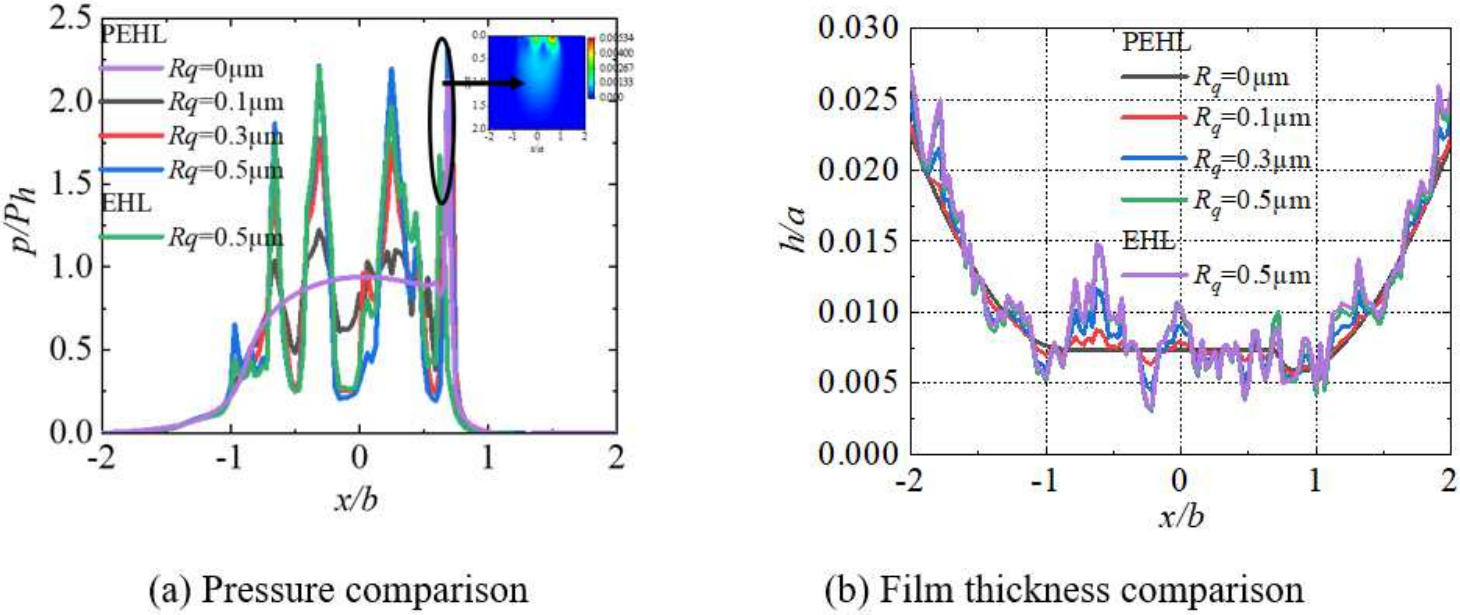

Figure 14

Influence of roughness on film thickness and pressure of the gas turbine bearing

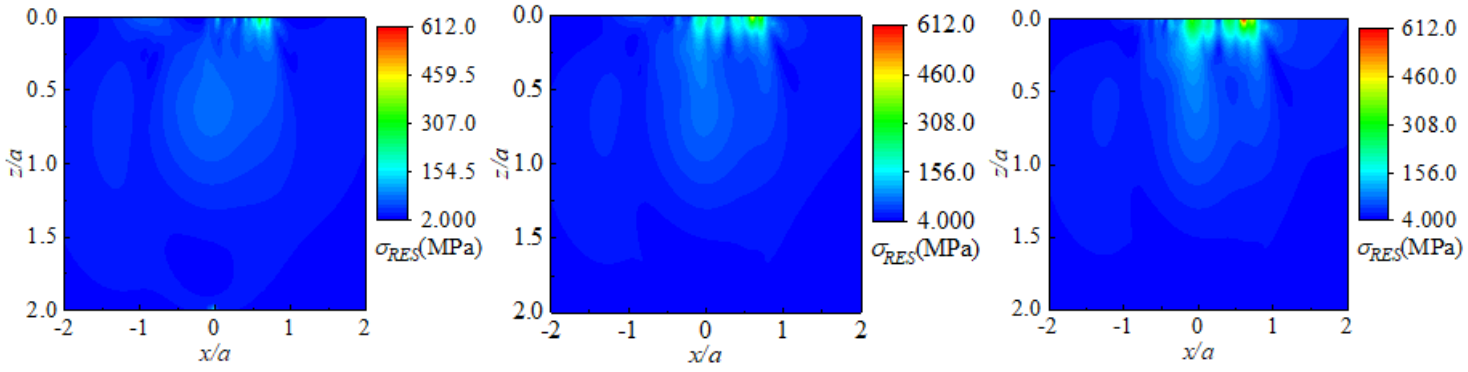

(a) $R_q = 0.1$ μm (b) $R_q = 0.3$ μm (c) $R_q = 0.5$ μm

Figure 15

The effect of the real roughness on the residual stress distribution of the gas turbine bearing

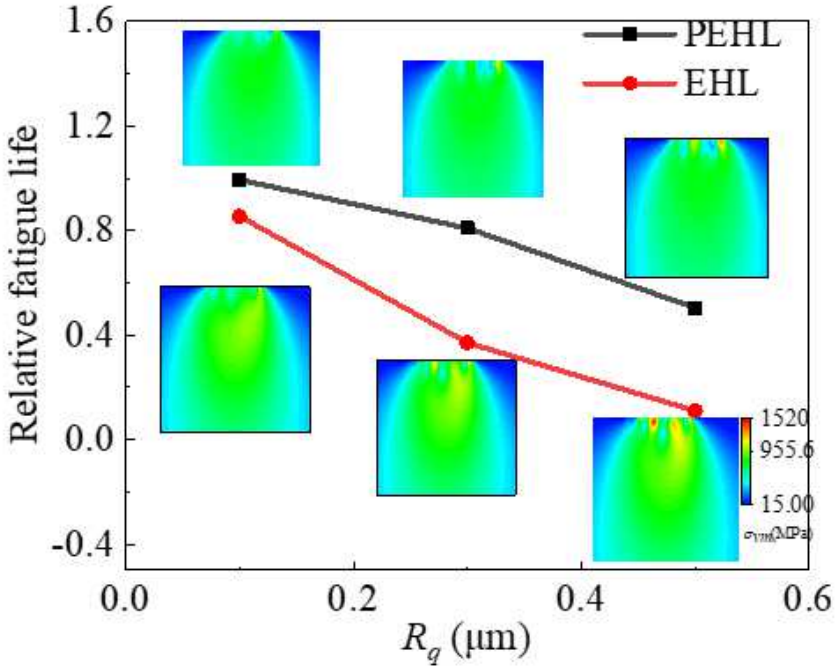

(a) Comparison of relative life

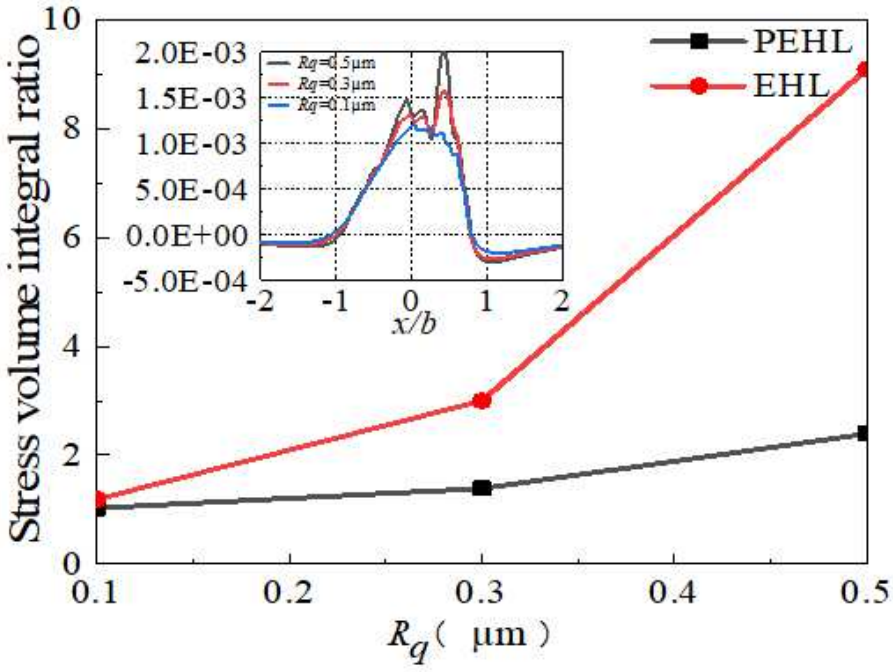

(b) Comparison of stress volume integral

Figure 16

Comparison of relative life and stress volume integral of PEHL and EHL under different roughness values